SUPPLEMENTAL FIGURES AND LEGENDS

A CCR2^{+} myeloid cell niche required for pancreatic β cell growth.

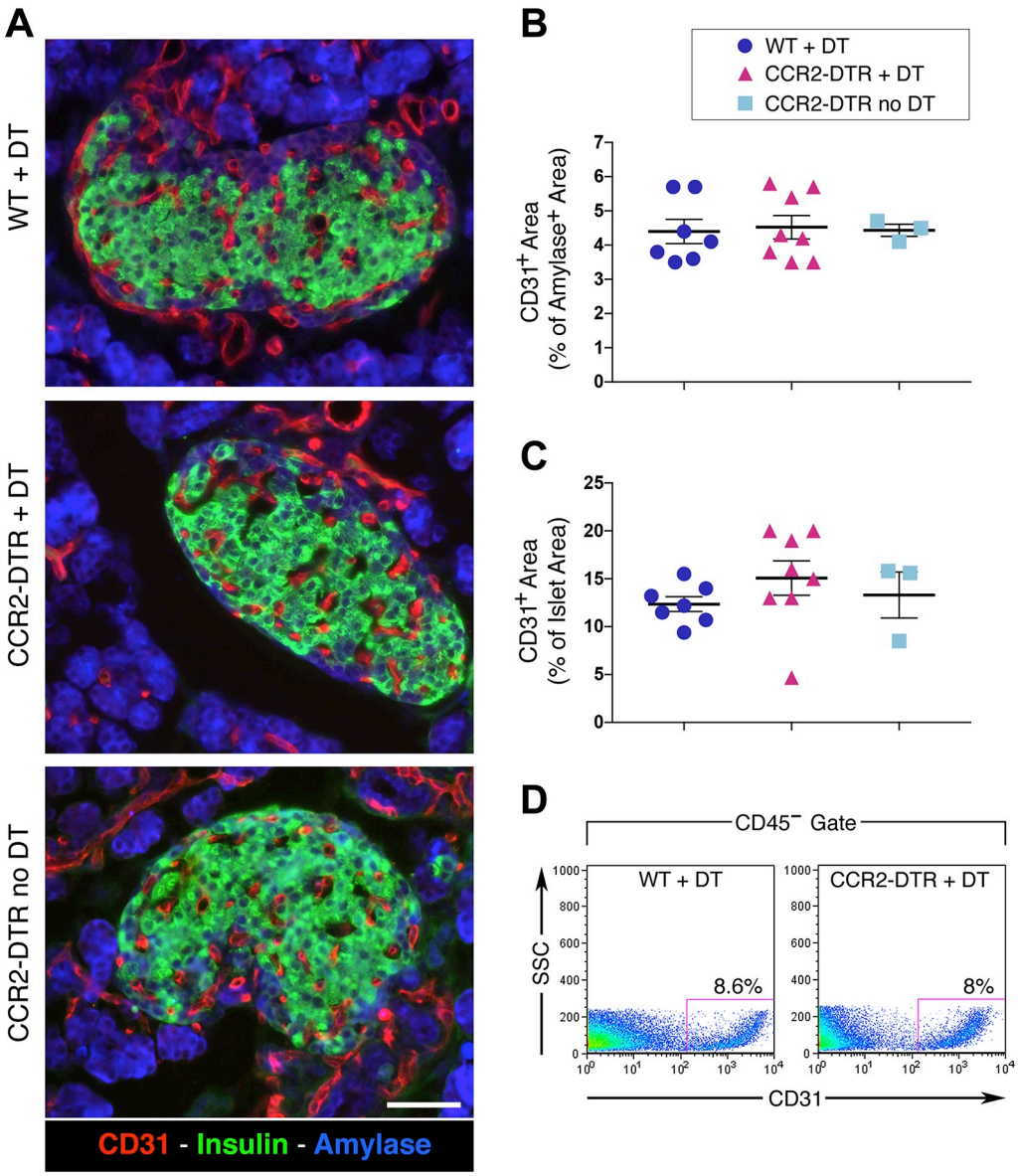

Figure S1. Effects of CCR2$^+$ cell loss on pancreatic vascular density. (A) Pancreatic sections of DT-treated and control P10 mice stained for the vascular marker CD31, insulin and amylase (n=3). (B) Morphometric analysis of tissue vascular densities detected in mice shown in (A). Transient peri-natal depletion of CCR2$^+$ cells does not negatively impact on the density of CD31$^+$ vascular beds in either the acinar or islet compartments. (D) Flow cytometric dot plots of pancreatic collagenase digests (pools of 2-3 tissues) immunostained for CD45 and CD31, showing a similar frequency of CD31$^+$ vascular cells in DT-treated WT and CCR2-DTR P10 pups. Cells were gated as CD45$^-$ to exclude from the analysis myeloid cells that may express low levels of CD31. Representative of n=2 experiments.

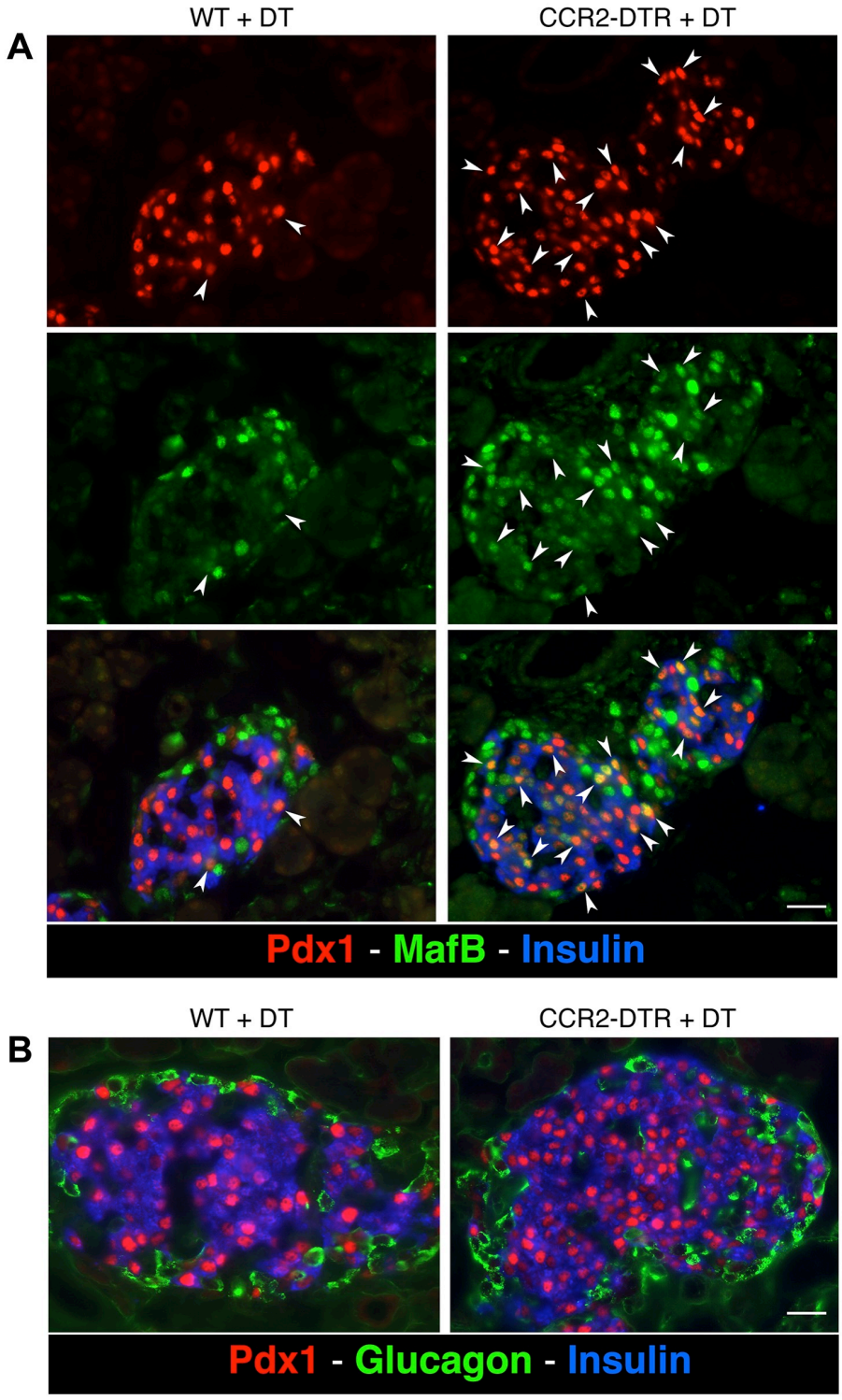

Figure S2. Increased co-expression of Pdx1 and MafB in β-cells of CCR2-depleted mice. (A) Pancreatic sections of DT-treated WT and CCR2-DTR P10 mice stained for Pdx1, MafB and Insulin, showing aberrant co-expression of Pdx1 and MafB in insulin-positive β-cells (arrowheads). (B) Pancreatic sections from the same animals stained for Pdx1, glucagon and insulin demonstrate appropriate exclusion of Pdx1 expression from most glucagon$^+$ α-cells. Representative of n=5.

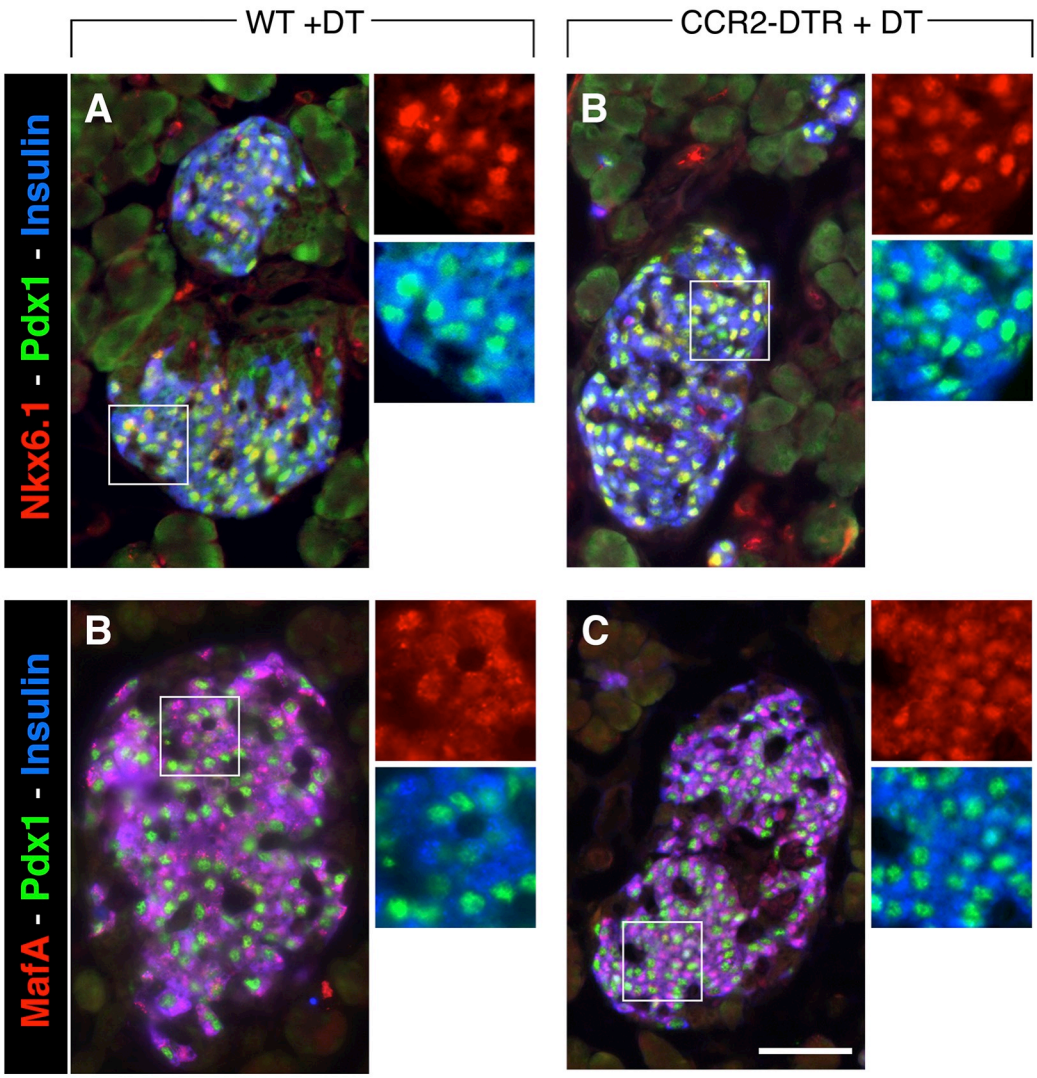

Figure S3. Adoptive transfer of DT-resistant myeloid cells prevents loss of NKX6.1 and MafA expression in pancreatic islets. (A-D) Pancreatic sections of DT-treated WT and CCR2-DTR P10 mice rescued with DT-resistant GR1+ cells show similar expression patterns of NKX6.1 (A-B) and MafA (C-D). Insets on the side show the predominant nuclear localization of NKX6.1 (A-B), and a mixed nuclear/cytoplasmic localization of MafA (C-D) in both mice. Representative of n=6.

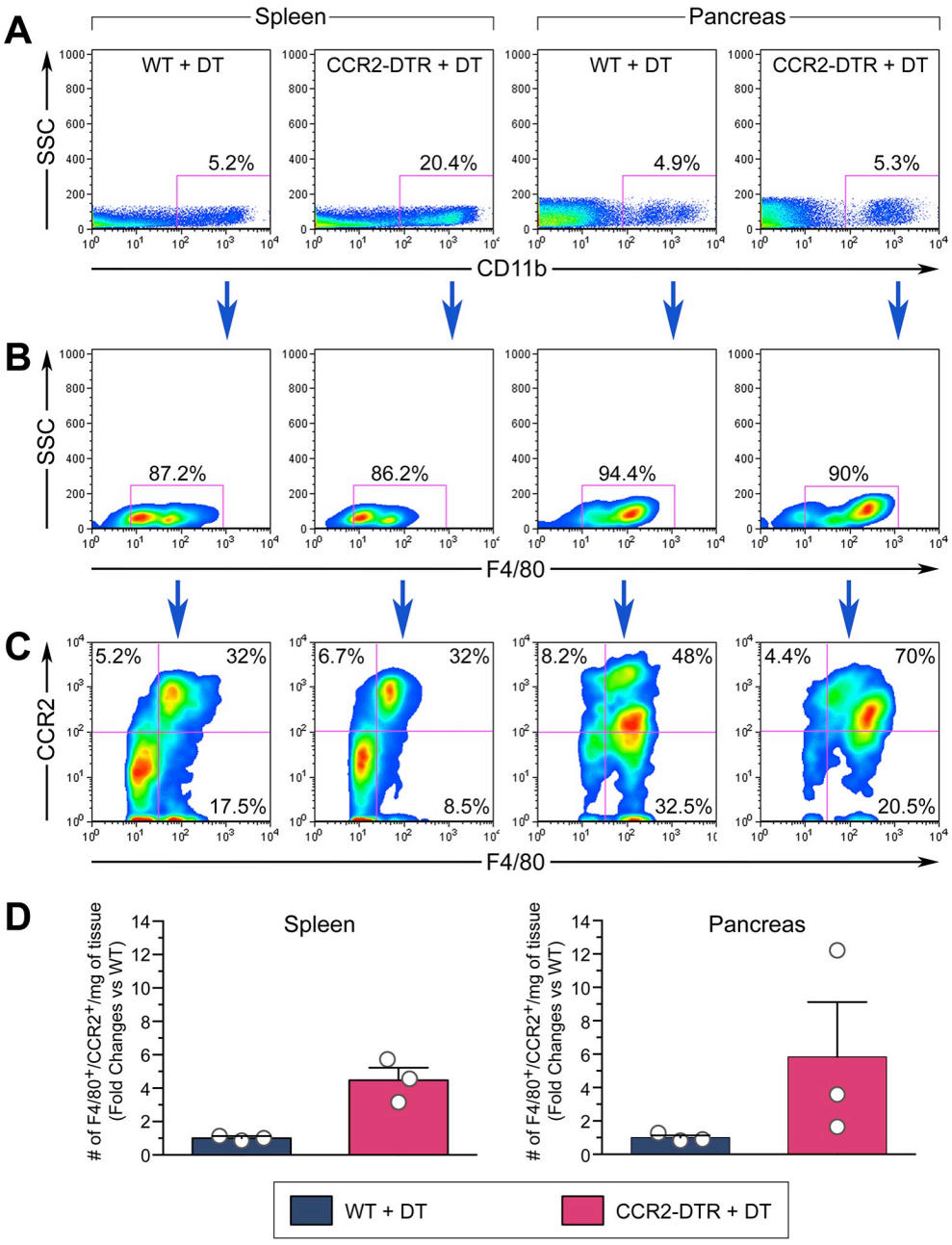

Figure S4. Spontaneous recovery of CCR2^{+} myeloid cells after DT withdrawal. (A-C) Flow cytometric analysis of splenic and pancreatic tissue samples from DT-treated WT and CCR2-DTR mice 6 days post-DT withdrawal (i.e. P14), immunostained for CD11b, F4/80 and CCR2 (representative of n=3). In (A), an increased frequency of myeloid CD11b^{+} cells is apparent in the spleen of CCR2-DTR mice recovering from DT treatment. (B) CD11b-gated cells showing splenic myeloid cells are mostly comprised of F480^{low} cells, whereas pancreatic subsets are mostly F480^{hi} cells, consistent with the presence of distinct monocytic and macrophage-like populations in the two tissue compartments. (C) F480-gated cells showing an increased frequency of F480^{hi}CCR2^{+} cells (upper-right quadrants) in the pancreas of CCR2-DTR mice. (D) Cumulative analysis of myeloid F480^{+}CCR2^{+} absolute counts derived from the flow cytometric data shown in B-C. Bars are mean±SD of n=3 tissue samples.